

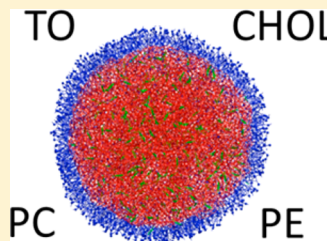
Lipid Structure in Triolein Lipid Droplets

Vitaly V. Chaban* and Himanshu Khandelia*

MEMPHYS – Center for Biomembrane Physics, Syddansk Universitet, Odense M., 5230, Denmark

S Supporting Information

ABSTRACT: Lipid droplets (LDs) are primary repositories of esterified fatty acids and sterols in animal cells. These organelles originate on the luminal or cytoplasmic side of endoplasmic reticulum (ER) membrane and are released to the cytosol. In contrast to other intracellular organelles, LDs are composed of a mass of hydrophobic lipid esters covered by phospholipid monolayer. The small size and unique architecture of LDs makes it complicated to study LD structure by modern experimental methods. We discuss coarse-grained molecular dynamics (MD) simulations of LD formation in systems containing 1-palmitoyl-2-oleoyl-*sn*-glycero-3-phosphocholine (POPC), 1-palmitoyl-2-oleoyl-*sn*-glycero-3-phosphoethanolamine (POPE), triolein (TO), cholesterol (CHOL), and water. We find that (1) there is more cholesterol in the LD core, than at the interface. (2) No crystallization occurs inside the LD core. (3) According to coarse-grained simulations, the presence of PE lipids at the interface has a little impact on distribution of components and on the overall LD structure. (4) The thickness of the lipid monolayer at the surface of the droplet is similar to the thickness of one leaflet of a bilayer. Computer simulations are shown to be a mighty tool to provide molecular-level insights, which are not available to the experimental techniques.



INTRODUCTION

Much attention in physical chemistry is now devoted^{1–4} to study molecular organization of lipid systems and lipid–water interfaces. Lipid droplets (LD)^{5–12} are omnipresent and dynamically regulated organelles found in various cell types throughout the complex life cycle of all eukaryotes. Lipids enter the cells as acids (free fatty acids) or sterols (free cholesterol, CHOL). High concentrations of lipids are deadly injurious to cells, whereas alcohols, such as diacylglycerols, are bioactive at low concentrations as signaling molecules. Evolution, therefore, had to develop an efficient mechanism to limit lipid concentrations, but retain their availability by coesterification of acids and alcohols into chemically inert neutral lipids (NL).^{6,13,14}

The majority of NL synthesis is routinely conducted at the endoplasmic reticulum (ER). Neutral lipids exhibit quite a limited solubility in the ER membrane bilayer. Neutral lipids are also immiscible with the hydrophilic intracellular environment. These properties result in lipid sequestration into cytoplasmic LDs, although the particular pathway is yet unknown. In recent years, the problem of LD biogenesis has received ever more attention, as pathological accumulation of NLs, both within cells and in serum, is a recognized harbinger of ill-health.^{15–17} Elevated cellular deposition of NLs typifies the epidemics of atherosclerosis and obesity.¹⁸ Similarly, elevated plasma levels of cholesteryl ester and triacylglycerols (TGLs) in low density lipoprotein particles represent independent risk factors for atherosclerosis. After adipocytes become saturated with lipids, other cells start accumulating NLs. It leads to diseases, such as diabetes and insulin resistance due to lipotoxicity at pancreatic β -cells and hepatocytes/myocytes.

There have been scattered reports investigating the biophysics and biochemistry of model TGL/phospholipid

mixtures. Pakkanen et al.^{13,19} pointed out fundamental differences between pure phosphatidylcholine bilayers and bilayers containing TO. Triolein induces unique alterations in the mechanical properties of POPC membranes as well as extraordinary conformational dynamics. Reluctance of TO-containing POPC membranes for lipid mixing with other membranes must be significant in biological systems. The authors indicated urgency of additional investigations of the role of triglycerides in the structure and functions of cellular membranes.

NMR studies^{20,21} have been applied to determine the maximum solubility of TGLs in model membranes containing mainly phospholipids and provided values within 3 mol % both in small unilamellar vesicles and in multilamellar vesicles of phosphatidylcholine lipids. In unilamellar vesicles, the solubility of TGLs is 1% if CHOL is present in 1:2 ratio with phospholipids and 0.15% if the ratio is 1:1.^{22,23} In all investigations, additional carbonyl peaks in the NMR spectra were obtained, as the concentration of TGLs was elevated above 4%. These peaks were typical of TGLs in the “oil” phase. Only 2–3 mol % of TGLs can be solubilized inside 1-palmitoyl-2-oleoyl-*sn*-glycero-3-phosphocholine (POPC) membranes and yet, more than 6–7 mol % are normally present within the cholesterol-containing membranes of living cells. Simulations showed that the excess TGL could be accumulated as a disordered aggregate in the middle of the lipid bilayer.²⁴

Computer simulations of lipid containing systems, such as atomistic and coarse-grained molecular dynamics simulations, Monte Carlo simulations and lower-resolution techniques,

Received: April 1, 2014

Revised: August 16, 2014

Published: August 18, 2014

allow to address numerous problems which cannot be solved using direct physical experiments. In particular, simulations can estimate the thickness of phospholipid monolayer, solubility of neutral lipids at the interface, nanoscale anisotropy of lipid distribution within the LD core. Lipid esters appear to preclude the presence of hydrophilic and amphiphilic molecules in the LD core. This supposition is consistent with electron microscopy observation, in which LDs are observed as featureless round objects with no internal structure. Such an image can, however, be deceptive and some differentiation may exist in the LD core. This paper addresses lipid arrangement in the core of LD as a function of phospholipid content.

The present manuscript reports coarse-grained molecular dynamics (MD) simulations of lipid droplets comprising TO, CHOL, POPC, and POPE in water. We investigate how lipids are packed inside LD and how the composition of phospholipid monolayer affects structure patterns of other lipids. The size of the simulated lipid droplets is chosen to correspond to minimum sizes of droplets which have been experimentally detected. We emphasize structure peculiarities of these relatively small LDs as a function of changeable monolayer composition. The reported results contribute to better understanding of LDs and provide assistance in the interpretation of biological experiments.

Prior molecular simulations of TGL containing systems have either focused on lipid emulsions^{25,26} or on lipoproteins. For instance, Vattulainen and co-workers reported structural and dynamical properties in the systems containing triolein and tripalmitin, with a particular attention to packing of TO molecules and their molecular conformations in the lipid environment.²⁷

The efficiency of lipases, and the rate of lipid droplet homeostasis (and consequently the presence of excess cholesterol and triglyceride which leads to diseased conditions) depends very much on the distribution of cholesterol and triglyceride inside the LD. The question “Does the lipid core have internal structure?” was posed as one of the key areas in the LD research in a recent review.¹¹ The internal structure of low density lipoprotein particles has undergone detailed investigation in literature,²⁸ but the distribution of core lipids in LDs remains to be explored. Computer simulations of lipid droplets provide atomistic-precision insights into their structure and transport properties, where necessary. These data are not available from experimental investigation or require unusual experimental setups. Radial distribution functions represent a powerful tool to characterize structure of the nanoscale objects with a molecular resolution.

■ COMPUTATIONAL METHODOLOGY

The list of the simulated systems is presented in Table 1. Systems 1–3, POPC-XX, contain TO and CHOL at fixed proportion, whereas POPC to POPE proportion is varied. The total amount of phospholipids was computed based on the experimentally determined area per phospholipid in bilayers, ca. 0.64 nm². Systems 4–5, PC-XX, in turn, contain fixed POPC to POPE proportion, but varying proportion to TO and CHOL lipids. The latter setups were implemented in order to investigate behavior of droplets, which do not possess enough phospholipids for a full coverage of the lipid–water interface. All unit cells were cubic. Each cell side was equal to ca. 30 nm, after the system density had stabilized. Figure 1 presents a snapshot of the simulated LD model (equilibrated structure).

Table 1. Designations and Compositions of the Simulated Systems^a

System	N(TO)	N(CHOL)	N(POPC)	N(POPE)	N(water)
POPC-100	3000	520	1942	0	125 044
POPC-75			1457	485	114 364
POPC-50			971	971	111 437
PC-75			1093	364	111 364
PC-25			364	121	111 364

^aPOPC-100, POPC-75 and POPC-50 (POPC-XX) systems differ by the POPC and POPE content. PC-75 and PC-25 (PC-XX) systems feature reduced number of phospholipids as compared to the full coverage. The hydrophobic core content is the same in all systems for a straightforward comparison.

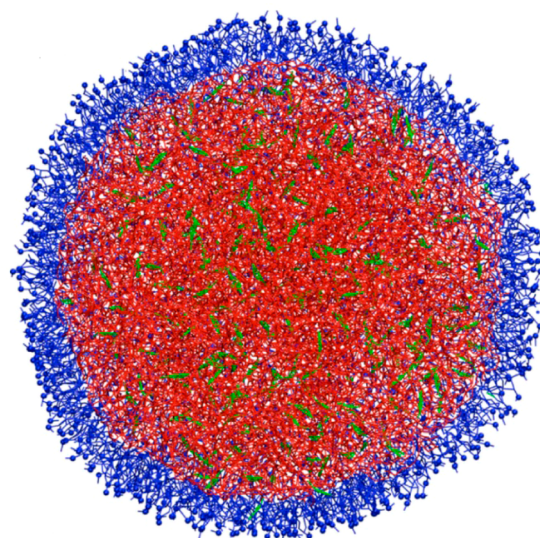


Figure 1. Cross-section of a lipid droplet solvated in water. TO molecules are red, CHOL molecules are green, POPC molecules are blue. Water is omitted for clarity. The snapshot was retrieved from the last time frame of the simulated POPC-100 system.

The trajectory was propagated using the GROMACS program suite.^{29–32} The particle types defined in the MARTINI coarse-grained force field^{33–37} were used to construct all objects (POPC, TO, CHOL, and water) in all systems. All equilibrium simulations were conducted in the constant temperature constant pressure ensemble at 333 K and 1 bar using the classical Berendsen thermostat and barostat with the relaxation times of 1.0 and 3.0 ps, respectively. Both electrostatic and Lennard-Jones (LJ) (12,6) constituents of the potential were modified according to the shifted force scheme with a shifting region from 0.0 to 1.2 nm for the Coulomb part and from 0.9 to 1.2 nm for the LJ part.³² The time-step for the integration of equations of motion was set to 0.02 ps. No intramolecular constraints, except those defined in the MARTINI force field,³⁷ were imposed. The intermediate coordinates were saved every 2 ns for the calculation of ensemble-averaged properties. Each system was simulated during 20 μ s of which the first five microseconds were disregarded as equilibration. With respect to dynamics acceleration coefficient in the MARTINI force field (ca. 4),³⁷ the simulation corresponds to 100 μ s of real (integrated) time, amounting to 400 μ s of the total simulated time in our work.

The topology files for POPC, POPE and CHOL molecules have been downloaded from <http://md.chem.rug.nl/cgmartini/>

index.php/force-field-parameters (maintained by Marrink group). The topology file for triolein was constructed by us using the default MARTINI atom types. This topology file can be retrieved from the Supporting Information.

The cluster analysis was performed using the single linkage approach. According to this approach, neighboring CHOL molecules form a cluster when any bead belonging to certain molecule is separated from any bead of neighboring molecule by less than a cutoff distance. The cutoff distance (0.75 nm) was selected with respect to the size of beads of the MARTINI coarse-grained force field. An alternative procedure would be to define a cluster only on the basis of a particular bead–bead contact referred to as a coordination center.

The distribution function with respect to the LD center-of-mass was defined to be consistent with conventional radial distribution function. That is, the value of this function at every point shows by how many times the numerical density of certain lipid exceeds the average numerical density of this same lipid in the simulated MD box. Using this knowledge, numerical or mass densities of molecules can be recovered, where necessary.

RESULTS AND DISCUSSION

The radius of gyration (Figure 2) was calculated as a root-mean-square distance of the object parts to the center-of-mass.

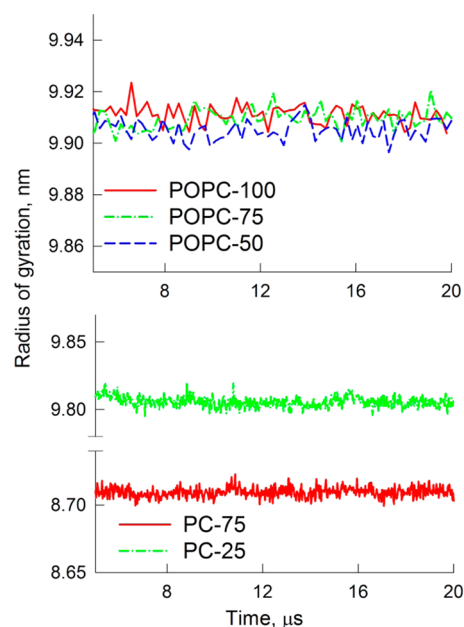


Figure 2. Radius of gyration of all simulated lipid droplets versus simulated time after system equilibration.

The radius of each droplet remains stable during the entire length of the simulation. The LDs with full coverage exhibit somewhat larger radii because they contain more lipids, whereas thermal fluctuations are ca. 0.01 nm in all cases. The sizes of the currently simulated LDs correspond to the smallest experimentally detected TGL droplets.

Figure 3 depicts selected radial distribution functions (RDFs) computed for the molecules in LDs. Interestingly, TO molecules are arranged in a very compact way; e.g., the first peak for the glycerol backbones is located at 0.55 nm. This peak exhibits a height of 19, suggesting that TO motion within the LD core is well correlated with neighboring TO molecules. The

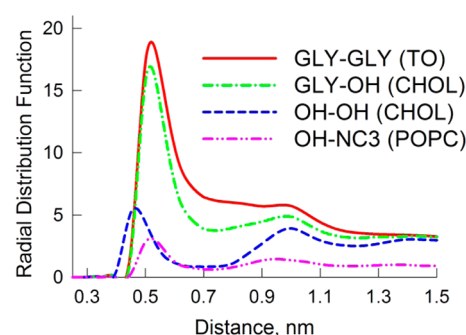


Figure 3. Radial distribution functions featuring key intermolecular interactions in lipid droplet: TO–TO glycerol backbone (red solid line), TO glycerol backbone–CHOL hydroxyl group (green dash-dotted line), CHOL hydroxyl group–CHOL hydroxyl group (blue dashed line), CHOL hydroxyl group–POPC choline group. The RDFs are derived for the POPC-75 system.

computed RDF for neighboring TO molecules is in general agreement with previously reported simulations of Hall et al.²⁷ Note that Hall et al. used an all-atomistic force field model. The atoms involved in calculations are not identical, although similar. Note that RDFs for TO molecules as well as for other particles do not decay to unity at the presented length scale (Figure 3), because density of lipid in TO core is higher than the average density of lipid in the MD box. The simulated lipid droplet systems are not homogeneous, while RDF normalization has been done with respect to the overall lipid density in the system. POPC headgroup–CHOL hydroxyl group RDF is relatively uniform. However, the first intermolecular peak is located at 0.55 nm, indicating that CHOL headgroup is able to directly approach phospholipid headgroup, which covers a lipid–water interface. Importantly, all RDFs exhibit the behavior characteristic of the liquid phase. This observation suggests that no crystallization occurs in the LD core.

The main physical reason for the phospholipid molecules (POPC, POPE, etc.) to be present at the LD–water interface is to minimize surface tension. The surface tension is especially high in case of relatively small LDs, as such simulated in the present work. The polar group of the phospholipid is oriented toward water, whereas hydrocarbon chains are oriented toward triolein molecules. Radial distribution function between the headgroup of phospholipids and triolein beads (Figure 4) is one of possible measures of phospholipid monolayer thickness. Note that unlike in Figure 3, the RDFs are computed between the phospholipid headgroup and the core lipid particles (TO, CHOL) closest to the phospholipid head groups, although all TO and CHOL particles are involved in the calculation. For the POPC-XX systems, the monolayer thickness is about 2 nm, which is the same as it would be in a fluid hydrated bilayer (the bilayer thickness is ca. 4 nm). This fact suggests that the phospholipids on the surface of the lipid droplet exhibit certain similarities to phospholipids in bilayers. This conclusion also follows from calculating lipid tail tilts (data not shown). The lipid tilt is defined as an angle between carbon–carbon bonds in the hydrophobic chains and the normal to LD. This property is easily derived in the case of the bilayer. For the PC-25 and PC-75 systems, however, the monolayer does not completely cover the lipid droplet. Figure 4 is an indication of how close TO molecules can approach the LD–water interface (or how close water can approach hydrophobic core of LD) during thermal motion. RDFs are larger than zero starting from 0.75 to

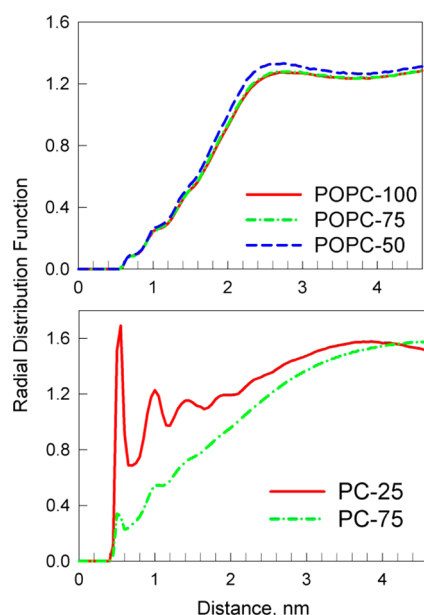


Figure 4. Radial distribution function computed between the phospholipid headgroup and core lipid particles (TO, CHOL) closest to the phospholipid head groups. All beads of core lipids and all beads of phospholipid head groups were involved in the calculation. Since phospholipid head groups and water molecules are in direct contact at the interface, these plots also indicate the separation between neutral lipids and water. One must account for diameters of beads in MARTINI (ca. 0.5 nm).

0.85 nm (POPC-100, POPC-75, POPC-50 systems) and from 0.45 to 0.50 nm (PC-25, PC-75 systems). Even in the case of fully covered interface, TO and water molecules approach quite closely. On the basis of the radii of the simulated beads, a direct TO-water contact would be manifested by the maximum at 0.45–0.5 nm. This maximum is indeed present in case of insufficiently covered interface (PC-25 system). The maximum is sharp but relatively small (1.7). The ability of the water phase to approach TO molecules is partly due to the ability of POPC layer to dissolve ca. 2 mol % of TO,^{20,21} and partly due to the incomplete phospholipid coverage of the lipid core in the PC-75 and PC-25 cases. Water molecules can sporadically cross the interface defended by the phospholipid head groups and approach TO, particularly at incomplete phospholipid coverage. Since this process is energetically unfavorable for the fully covered interfaces, the density of water near TO in these systems is smaller than unity (Figure 4, top). The information obtained from Figure 4 is very important to understand how nascent LDs fuse, even though they are fully defended by a phospholipid monolayer. Without an ability of triolein molecules to approach an aqueous phase, the driving force for LD fusion would remain unknown, since hydrophobe molecules do not attract to one another directly at the separation of ca. 2 nm (monolayer thickness). Because of TO solubility in the phospholipid monolayer, LD fusion and hence growth becomes possible.

Radial distribution function computed for hydroxyl group of CHOL and water is given in Figure S1, Supporting Information. The RDF was computed in the POPC-75 (fully covered LD) and PC-25 (lack of phospholipids) systems. CHOL molecules are present at the interface (the first peak) and within the monolayer (the second and the third peaks). However, the heights of these peaks are smaller than unity,

since the majority of CHOL molecules are in the LD core. Compare our conclusions with Figure 1. The partially covered LD contains more CHOL molecules at the interface, since they act as a surfactant.

In order to understand packing of all lipids constituting the lipid droplet with respect to one another, we computed distribution functions of each lipid to geometrical center of LD (Figure 5). The hydrophobic core of LD is formed by TO and

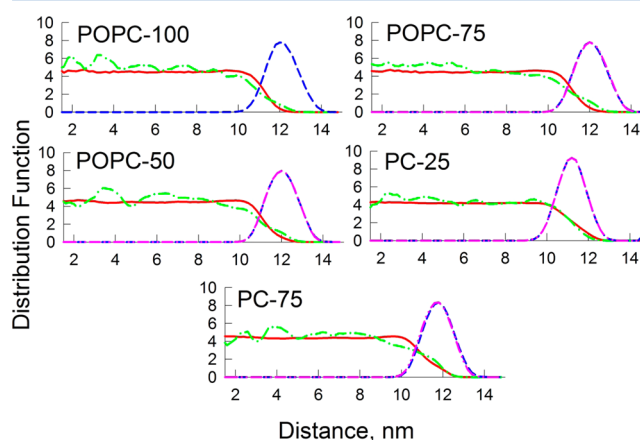


Figure 5. Distributions of lipid radial densities as a function of distance from the geometrical center of LD in all simulated systems. The geometrical center of LD was recomputed at every recorded molecular frame. TO density is solid red line, CHOL density is dash-dotted green line, POPC density is dashed blue line, and POPE density is dash-dot-dotted pink line.

CHOL molecules. CHOL and TO molecules are well miscible. This feature allows for LD to transfer CHOL not only in the outer region, but also in the inner region. The LD–water interface is predominantly populated by POPC and POPE molecules. However, certain smaller fraction of TO and CHOL is also observed (note the intersecting lines). The droplets with reduced number of phospholipids (PC-75, PC-25) are somewhat smaller than the fully covered droplets (POPC-100, POPC-75, POPC-50). No observable difference between POPC and POPE at the interface is found. It may be partially due to relatively small difference between numerical parameters for PC and PE head groups in the applied coarse-grained force field. However, we believe that MARTINI force field provides qualitatively sound results. Since the number of phospholipids is exactly sufficient to cover an entire LD–water interface area, no excess phospholipids are present. Therefore, there is no competition between phospholipids for the place at the interface and there is no difference in their location with respect to the LD geometrical center.

Figure 6 depicts distribution of CHOL clusters in the simulated LDs. More than 80 mol % of CHOL exist as lone molecules surrounded by TO molecules, i.e., form a real solution of CHOL in TO. Here, 15 mol % of CHOL molecules form dimers, whereas larger molecular aggregates are under-represented. The probability of their formation is lower than 2%. It must be noted that CHOL content in certain kinds of natural LDs is higher than in the LDs simulated in this work (9.5 mol % in the systems with full phospholipid coverage). In those systems, the content of CHOL is likely to exceed its solubility in TO. The solubility of CHOL in an oil phase as well as an effect of aqueous phase has already been reported.³⁸

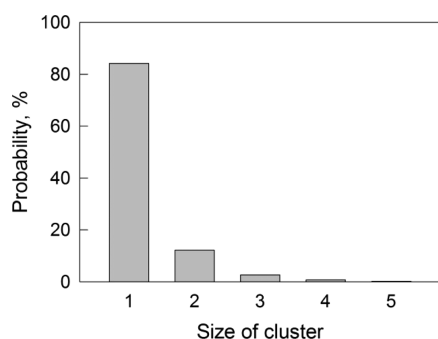


Figure 6. Sizes of clusters formed by CHOL in the core of LD. The depicted distribution corresponds to the POPC-75 system. All simulated systems exhibit similar CHOL cluster distributions (within the error bars). Note that TO/CHOL ratio is constant in all the simulated systems.

Therefore, large molecular aggregates involving CHOL or even an additional CHOL phase within the droplet may be expected.

SAMPLING ISSUES

Sampling of lipid-containing systems is a keynote issue, since these systems exhibit high shear viscosity and small self-diffusion coefficients of the components. In order to rely on the simulation results, ergodicity of simulation should be ensured; i.e., an average over the sampled time region should be equal to an average over sampled spatial region. After location of the free energy minimum, the system must visit most states of the phase space at given temperature and pressure.

The coarse-grained models possess an advantage over all-atom force field models in context of proper sampling of phase space. The process of coarse-graining is a substitution of atoms by larger-size beads, resulting in the decrease of total degrees of freedom per system. The reduction of degrees of freedom means a simpler potential energy surface, which must be sampled during molecular dynamics. Therefore, in addition to a possibility of using larger integration time-step, the coarse-grained representations accelerate sampling speed. The payoff for the mentioned acceleration is a limited possibility to investigate metastable states, such as superheated and supercooled liquids, supersaturated solutions, etc. Nonequilibrium phenomena should also be treated with a high caution.

Diffusion constants can be directly retrieved from the MD trajectory. As such, they constitute an important measure of how well the simulated time corresponds to the simulated energy surface. The diffusion coefficients for TO, CHOL, POPC, and POPE molecules in the investigated systems are 6, 11, 9, and $9 \times 10^{-11} \text{ m}^2 \text{ s}^{-1}$, respectively. On the basis of these molecular mobilities, one easily estimates that each individual TO, CHOL, POPC, and POPE molecule diffuses by 24.5, 33.2, 30, and 30 nm, respectively, starting from the beginning of MD simulation and finishing at time equal to 20 μs . These distances are comparable to the diameter of each LD is ca. 20 nm. To rephrase, each simulated lipid is able to sample virtually the entire volume of the object, which provides solid evidence for proper sampling. This estimate does not account for symmetry considerations, which will further decrease minimum necessary sampling times, as all TO and CHOL molecules in the core are physically identical.

Note that reported self-diffusion coefficients are provided for information on the genuine dynamics of the simulated systems. These coefficients should not be directly compared to

experimental values and to diffusions coefficients derived from all-atomistic molecular dynamics studies. The limitations concerning simulated dynamics and simulated time scales can be retrieved from the original paper introducing the MARTINI force field.³⁷

CONCLUSIONS

Our study provides answers to several important questions existing in the current LD research. As pointed out in the recent review article,¹¹ it is unknown until now whether free CHOL exists only at the surface of LD or also in the core. Our study provides evidence that CHOL exists throughout the LD, whereas the extent of phospholipid coverage does not affect this observation. Over 80% CHOL molecules exist as lone molecules in TO medium, whereas 15% form dimers. In case of larger content of CHOL and steryl esters (beyond their solubility limit in TO), it is completely possible that they form concentric layers between the TO-rich core¹¹ and the phospholipid cap.

ASSOCIATED CONTENT

Supporting Information

Figure S1 depicting radial distribution functions computed for polar moiety (hydroxyl group) of CHOL and water beads and the newly constructed topology file for triolein molecule (18 MARTINI beads). This material is available free of charge via the Internet at <http://pubs.acs.org>.

AUTHOR INFORMATION

Corresponding Authors

*(V.V.C.) E-mail: vvchaban@gmail.com.

*(H.K.) E-mail: hkhandel@memphys.sdu.dk.

Notes

The authors declare no competing financial interest.

ACKNOWLEDGMENTS

The discussed computations have been carried at the SDU node of the Danish Center for Scientific Computing. This research has been funded by a Lundbeckfonden Young Investigator Grant (Khandelia).

REFERENCES

- (1) Staples, E.; Penfold, J.; Tucker, I. Adsorption of Mixed Surfactants at the Oil-Water Interface. *J. Phys. Chem. B* **2000**, *104*, 606–614.
- (2) Vazdar, M.; Wernersson, E.; Khabiri, M.; Cwiklik, L.; Jurkiewicz, P.; Hof, M.; Mann, E.; Kolusheva, S.; Jelinek, R.; Jungwirth, P. Aggregation of Oligoarginines at Phospholipid Membranes: Molecular Dynamics Simulations, Time-Dependent Fluorescence Shift, and Biomimetic Colorimetric Assays. *J. Phys. Chem. B* **2013**, *117*, 11530–11540.
- (3) Shillcock, J. C.; Lipowsky, R. The Computational Route from Bilayer Membranes to Vesicle Fusion. *J. Phys.-Condens Mat* **2006**, *18*, S1191–S1219.
- (4) Risselada, H. J.; Mark, A. E.; Marrink, S. J. Application of Mean Field Boundary Potentials in Simulations of Lipid Vesicles. *J. Phys. Chem. B* **2008**, *112*, 7438–7447.
- (5) Sturley, S. L.; Hussain, M. M. Thematic Review Series: Lipid Droplet Synthesis and Metabolism: From Yeast to Man Lipid Droplet Formation on Opposing Sides of the Endoplasmic Reticulum. *J. Lipid Res.* **2012**, *53*, 1800–1810.
- (6) Kuhnlein, R. P. Thematic Review Series: Lipid Droplet Synthesis and Metabolism: From Yeast to Man Lipid Droplet-Based Storage Fat Metabolism in *Drosophila*. *J. Lipid Res.* **2012**, *53*, 1430–1436.

- (7) Wigglesworth, Vb Catalysomes or Enzyme Caps on Lipid Droplets - an Intracellular Organelle. *Nature* **1966**, *210*, 759–8.
- (8) Beckman, M. Cell Biology - Great Balls of Fat. *Science* **2006**, *311*, 1232–1234.
- (9) Zimmermann, R.; Strauss, J. G.; Haemmerle, G.; Schoiswohl, G.; Birner-Gruenberger, R.; Riederer, M.; Lass, A.; Neuberger, G.; Eisenhaber, F.; Hermetter, A.; et al. Fat Mobilization in Adipose Tissue Is Promoted by Adipose Triglyceride Lipase. *Science* **2004**, *306*, 1383–1386.
- (10) Fujimoto, T.; Ohsaki, Y.; Cheng, J.; Suzuki, M.; Shinohara, Y. Lipid Droplets: A Classic Organelle with New Outfits. *Histochem. Cell Biol.* **2008**, *130*, 263–279.
- (11) Ohsaki, Y.; Suzuki, M.; Fujimoto, T. Open Questions in Lipid Droplet Biology. *Chem. Biol.* **2014**, *21*, 86–96.
- (12) Thiam, A. R.; Farese, R. V.; Walther, T. C. The Biophysics and Cell Biology of Lipid Droplets. *Nat. Rev. Mol. Cell Bio* **2013**, *14*, 775–786.
- (13) Pakkanen, K. I.; Duelund, L.; Qvortrup, K.; Pedersen, J. S.; Ipsen, J. H. Mechanics and Dynamics of Triglyceride-Phospholipid Model Membranes: Implications for Cellular Properties and Function. *Bba-Biomembranes* **2011**, *1808*, 1947–1956.
- (14) Lahdesmaki, K.; Ollila, O. H. S.; Koivuniemi, A.; Kovanen, P. T.; Hyvonen, M. T. Membrane Simulations Mimicking Acidic Ph Reveal Increased Thickness and Negative Curvature in a Bilayer Consisting of Lysophosphatidylcholines and Free Fatty Acids. *Bba-Biomembranes* **2010**, *1798*, 938–946.
- (15) Pan, X. Y.; Wilson, M.; McConville, C.; Brundler, M. A.; Arvanitis, T. N.; Shockcor, J. P.; Griffin, J. L.; Kauppinen, R. A.; Peet, A. C. The Lipid Composition of Isolated Cytoplasmic Lipid Droplets from a Human Cancer Cell Line, Be(2)M17. *Mol. Biosyst* **2012**, *8*, 1694–1700.
- (16) Bozza, P. T.; Viola, J. P. B. Lipid Droplets in Inflammation and Cancer. *Prostag. Leukotr. Ess.* **2010**, *82*, 243–250.
- (17) Bozza, P. T.; Viola, J. P. B. Biogenesis and Functions of Lipid Droplets in Inflammation and Cancer. *Int. J. Mol. Med.* **2009**, *24*, S52–S52.
- (18) McDonough, P. M.; Agustin, R. M.; Ingermanson, R. S.; Loy, P. A.; Buehrer, B. M.; Nicoll, J. B.; Prigozhina, N. L.; Mikic, I.; Price, J. H. Quantification of Lipid Droplets and Associated Proteins in Cellular Models of Obesity Via High-Content/High-Throughput Microscopy and Automated Image Analysis. *Assay Drug Dev. Technol.* **2009**, *7*, 440–460.
- (19) Pakkanen, K. I.; Duelund, L.; Vuento, M.; Ipsen, J. H. Phase Coexistence in a Triolein-Phosphatidylcholine System. Implications for Lysosomal Membrane Properties. *Chem. Phys. Lipids* **2010**, *163*, 218–227.
- (20) Hamilton, J. A. Interactions of Triglycerides with Phospholipids - Incorporation into the Bilayer Structure and Formation of Emulsions. *Biochemistry* **1989**, *28*, 2514–2520.
- (21) Hamilton, J. A.; Small, D. M. Solubilization and Localization of Triolein in Phosphatidylcholine Bilayers - a C-13 Nmr-Study. *Proc. Natl. Acad. Sci. U.S.A.—Biol.* **1981**, *78*, 6878–6882.
- (22) Spooner, P. J. R.; Small, D. M. Effect of Free-Cholesterol on Incorporation of Triolein in Phospholipid-Bilayers. *Biochemistry* **1987**, *26*, 5820–5825.
- (23) Spooner, P. J. R.; Small, D. M. The Effect of Free-Cholesterol on the Solubility of Triolein in Phospholipid-Bilayers. *Biophys. J.* **1987**, *51*, A188–A188.
- (24) Khandelia, H.; Duelund, L.; Pakkanen, K. I.; Ipsen, J. H. Triglyceride Blisters in Lipid Bilayers: Implications for Lipid Droplet Biogenesis and the Mobile Lipid Signal in Cancer Cell Membranes. *PLoS One* **2010**, *5*, e12811.
- (25) Huynh, L.; Neale, C.; Pomes, R.; Allen, C. Computational Approaches to the Rational Design of Nanoemulsions, Polymeric Micelles, and Dendrimers for Drug Delivery. *Nanomed. Nanotechnol.* **2012**, *8*, 20–36.
- (26) Hennere, G.; Prognon, P.; Brion, F.; Rosilio, V.; Nicolis, I. Molecular Dynamics Simulation of a Mixed Lipid Emulsion Model: Influence of the Triglycerides on Interfacial Phospholipid Organization. *J. Mol. Struct.—THEOCHEM* **2009**, *901*, 174–185.
- (27) Hall, A.; Repakova, J.; Vattulainen, I. Modeling of the Triglyceride-Rich Core in Lipoprotein Particles. *J. Phys. Chem. B* **2008**, *112*, 13772–13782.
- (28) Orlova, E. V.; Sherman, M. B.; Chiu, W.; Mowri, H.; Smith, L. C.; Gotto, A. M. Three-Dimensional Structure of Low Density Lipoproteins by Electron Cryomicroscopy. *Proc. Natl. Acad. Sci. U.S.A.* **1999**, *96*, 8420–8425.
- (29) Hess, B.; Kutzner, C.; van der Spoel, D.; Lindahl, E. Gromacs 4: Algorithms for Highly Efficient, Load-Balanced, and Scalable Molecular Simulation. *J. Chem. Theory Comput.* **2008**, *4*, 435–447.
- (30) Lindahl, E.; Hess, B.; van der Spoel, D. Gromacs 3.0: A Package for Molecular Simulation and Trajectory Analysis. *J. Mol. Model* **2001**, *7*, 306–317.
- (31) van der Spoel, D.; Hess, B. Gromacs-the Road Ahead. *Wires Comput. Mol. Sci.* **2011**, *1*, 710–715.
- (32) Van der Spoel, D.; Lindahl, E.; Hess, B.; Groenhof, G.; Mark, A. E.; Berendsen, H. J. C. Gromacs: Fast, Flexible, and Free. *J. Comput. Chem.* **2005**, *26*, 1701–1718.
- (33) Wassenaar, T. A.; Ingolfsson, H. I.; Priess, M.; Marrink, S. J.; Schafer, L. V. Mixing Martini: Electrostatic Coupling in Hybrid Atomistic-Coarse-Grained Biomolecular Simulations. *J. Phys. Chem. B* **2013**, *117*, 3516–3530.
- (34) de Jong, D. H.; Singh, G.; Bennett, W. F. D.; Arnarez, C.; Wassenaar, T. A.; Schafer, L. V.; Periole, X.; Tieleman, D. P.; Marrink, S. J. Improved Parameters for the Martini Coarse-Grained Protein Force Field. *J. Chem. Theory Comput* **2013**, *9*, 687–697.
- (35) Yesylevskyy, S. O.; Schafer, L. V.; Sengupta, D.; Marrink, S. J. Polarizable Water Model for the Coarse-Grained Martini Force Field. *PLoS Comput. Biol.* **2010**, *6*, e1000810.
- (36) Monticelli, L.; Kandasamy, S. K.; Periole, X.; Larson, R. G.; Tieleman, D. P.; Marrink, S. J. The Martini Coarse-Grained Force Field: Extension to Proteins. *J. Chem. Theory Comput* **2008**, *4*, 819–834.
- (37) Marrink, S. J.; Risselada, H. J.; Yefimov, S.; Tieleman, D. P.; de Vries, A. H. The Martini Force Field: Coarse Grained Model for Biomolecular Simulations. *J. Phys. Chem. B* **2007**, *111*, 7812–7824.
- (38) Jandacek, R. J.; Webb, M. R.; Mattson, F. H. Effect of an Aqueous Phase on Solubility of Cholesterol in an Oil Phase. *J. Lipid Res.* **1977**, *18*, 203–210.